Spectral and near-field characteristics of induced microseismicity

David W. Eaton*, Farshid Forouhideh
Department of Geoscience, University of Calgary, Calgary, Canada

Mirko van der Baan
Department of Physics, University of Alberta, Edmonton, Canada

Summary

Microseismic methods have emerged as an important tool for monitoring fluid processes at the reservoir scale, especially for hyrofrac treatment of tight gas reservoirs. The signals produced by microseismic events carry significant information about the characteristics of the source, as well as the effects of wavefield propagation between the source and receiver. If propagation effects can be estimated and removed, inferences can be made about the source such as the style and dimensions of rupture, or stress drop. Moreover, if the path length is less than a few seismic wavelengths (10's m), the recorded wavefield is expected to include exotic near-field terms with atypical pulse characteristics that might inhibit conventional analysis. Such near-field terms could be important if geophones are deployed within the treatment well, rather than in a separate observation well. This theoretical study considers the potential to extract additional information from microseismic observations, in both near- and far-field recording environments.

Source spectrum and stress drop

A simple model for shear displacement due to slip on a circular crack is given by

$$d(t) = D\left[1 - (1 + t/\tau)e^{-t/\tau}\right] \quad , \tag{1}$$

where D is the net displacement and τ is called the rise-time parameter. Figure 1a depicts this ramp-like function, which increases smoothly from zero to the full displacement over about 5 rise times. The far-field displacement spectrum of elastic waves radiated from such a source is given by (Beresnev, 2001)

$$\tilde{d}(\omega) = \frac{M_0}{1 + \left(\dfrac{\omega}{\omega_c}\right)^2} \quad , \tag{2}$$

where ~ denotes the Fourier transform, $\omega = 2\pi f$ and $\omega_c \equiv 1/\tau$ is called the angular corner frequency. The corresponding velocity spectrum is given by

$$v(\omega) = \frac{M_0\omega}{1 + \left(\dfrac{\omega}{\omega_c}\right)^2} \quad . \tag{3}$$

These canonical displacement and velocity spectra are graphed in Figs. 1b and 1c. Since geophones measure ground velocity, the velocity spectrum gives a representation of the expected spectral signal content from a microseismic event. We see that the velocity spectrum exhibits a smooth maximum that peaks at the corner frequency, $f_c = \omega/2\pi$. The displacement spectrum, derived easily from the velocity spectrum by division by ω, exhibits an asymptotic low-frequency limit that is equal to the seismic moment (M_0). In practice, direct estimation of M_0 by spectral analysis requires careful data processing to correct for instrument response and path effects (e.g. Dineva et al., 2007).
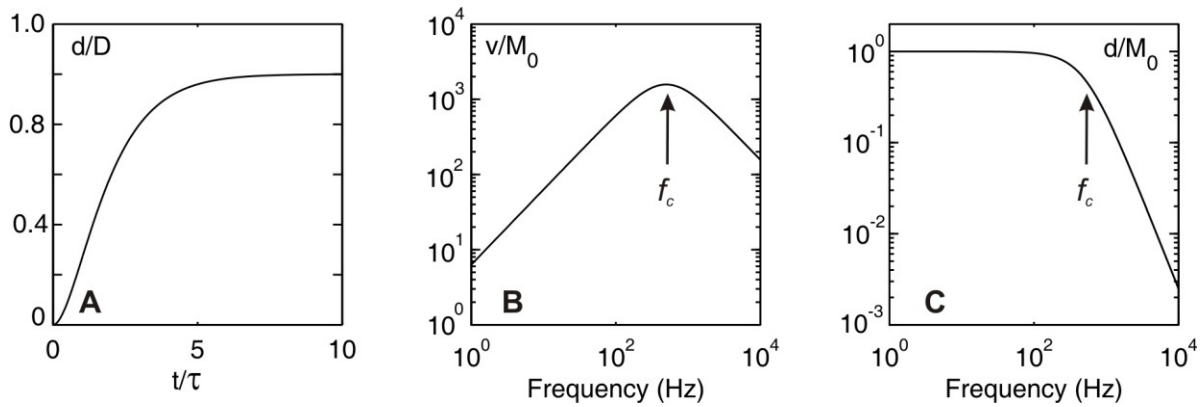
Fig. 1. A) Simple model for displacement on a circular crack, as described by equation 1. B) Theoretical amplitude spectrum for ground velocity, normalized by the seismic moment (M_0). The corner frequency (fc) coincides with the peak in the spectrum. C) Theoretical spectrum of normalized ground displacement. The low-frequency asymptotic limit defines M_0.

Once the corner frequency is determined from the peak in the velocity spectrum, it can then be used to estimate the radius of a circular fault (Brune 1970, 1971)

$$R \approx 2.34 \frac{\beta}{\omega_c} \quad , \tag{4}$$

where β is the shear-wave velocity of the medium. The Brune source radius provides a crude estimate of fracture half length, although caution is required in the interpretation of this parameter (Beresnev, 2001). Similarly, we can use the corner frequency to provide a crude estimate of the stress drop ($\Delta\sigma$, the average difference between stress before and after the slip event) using

$$\omega_c \approx 2.34 \times 2\beta \left(\frac{\Delta\sigma}{M_0}\right)^{1/3} \quad . \tag{5}$$

In earthquake studies, the stress drop is often used as a proxy for fault strength. Finally, the seismic moment is related to by the relation

$$M_w = \frac{2}{3}\log_{10}(M_0) - 6.03 \tag{6}$$

where M_W is the moment magnitude and M_0 is in units of N-m. Figure 2a shows the theoretical corner frequency computed using equations (5) and (6) for magnitudes in the typical range for hydrofrac monitoring studies (-3 to 0) and values of stress drop ranging from very weak (10 bars = 1 MPa) to very strong (200 bars = 20 MPa). We remark that the lower range of corner frequency, applicable to large events and/or weak slip systems, should be measurable using commonly used borehole microseismic acquisition systems. In principle, the determination of corner frequency and M_0, coupled with a priori knowledge of background shear-wave velocity, should enable estimation of Brune source radius (Fig. 2b) using equation (4) and stress drop using equation (5). The potential diagnostic and/or comparative value of these parameters is currently being investigated for a number of case studies.
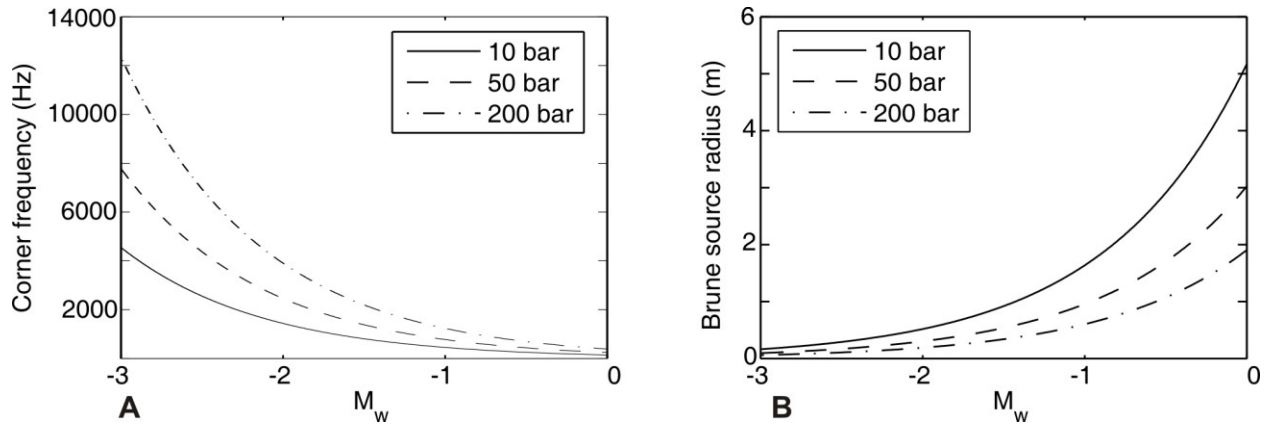
Fig. 2. A) Predicted value of corner frequency (f_c) versus moment magnitude for various values of stress drop that range from very weak (10 bars) to very strong (200 bars) slip systems. B) Brune source radius versus moment magnitude, showing a range from a few cm to 5m.

Effects of near-field source terms

Seismologists are accustomed to modeling waveforms using ray theory and/or simple convolution models. These approaches are known to break down for complex media. In addition, these models will lose applicability in the near-field (i.e., measurements made within a few seismic wavelengths of the source location). The latter could arise, for example, in hydrofrac monitoring surveys where the same well is used for both observation and injection.

To investigate near-field phenomena, we turn to the full elastodynamic Green's function for a homogeneous elastic medium. The nth component of ground velocity due to a point-dislocation source may be written as:

$$v_n(t) = \frac{a_{pq}}{4\pi\rho r^4} \int_{r/\alpha}^{r/\beta} \tau M_{pq}\dot{s}(t-\tau)d\tau + \frac{b_{pq}}{4\pi\rho\alpha^2 r^2}M_{pq}\dot{s}\left(t-\frac{r}{\alpha}\right) + \frac{c_{pq}}{4\pi\rho\beta^2 r^2}M_{pq}\dot{s}\left(t-\frac{r}{\beta}\right)$$

$$+ \frac{d_{pq}}{4\pi\rho\alpha^3 r}M_{pq}\ddot{s}\left(t-\frac{r}{\alpha}\right) + \frac{e_{pq}}{4\pi\rho\beta^3 r}M_{pq}\ddot{s}\left(t-\frac{r}{\beta}\right) \quad , \tag{7}$$

where r is distance, α, β and ρ are the P- and S-wave velocity and density of the medium, M_{pq} is the moment tensor, $s(t)$ is the source time function and a_{pq}, b_{pq}, c_{pq}, d_{pq} and e_{pq} are geometrical terms (see Aki and Richards, 1980, p. 79 for details). The first three terms in this expression represent near-field terms that decay as $1/r^4$ and $1/r^2$ respectively. The last two terms decay as $1/r$ and represent far-field P- and S-waves.

Figure 3 shows the calculated seismic pulse using equation (7) for a double-couple mechanism for three distance ranges (10, 50 and 200 m). The source time function is given by equation (1), using a corner frequency of 320 Hz corresponding to a large microseismic event (Fig. 2a). The backround medium has P- and S-wave velocities of 4000 m/s and 2000 m/s, respectively, corresponding to wavelengths of 12.5 and 6.25 m for the peak spectral value. At 200 m distance, typical for microseismic data from a remote observation well, the near-field terms are negligible and P- and S-waves arrive with distinct pulses. At 50 m, near-field terms are subtly expressed via a low-frequency signal between the P- and S-wave arrivals. At 10 m distance, near-field terms are dominant. The pulse shape and polarity differ markedly from the far-field waveforms.
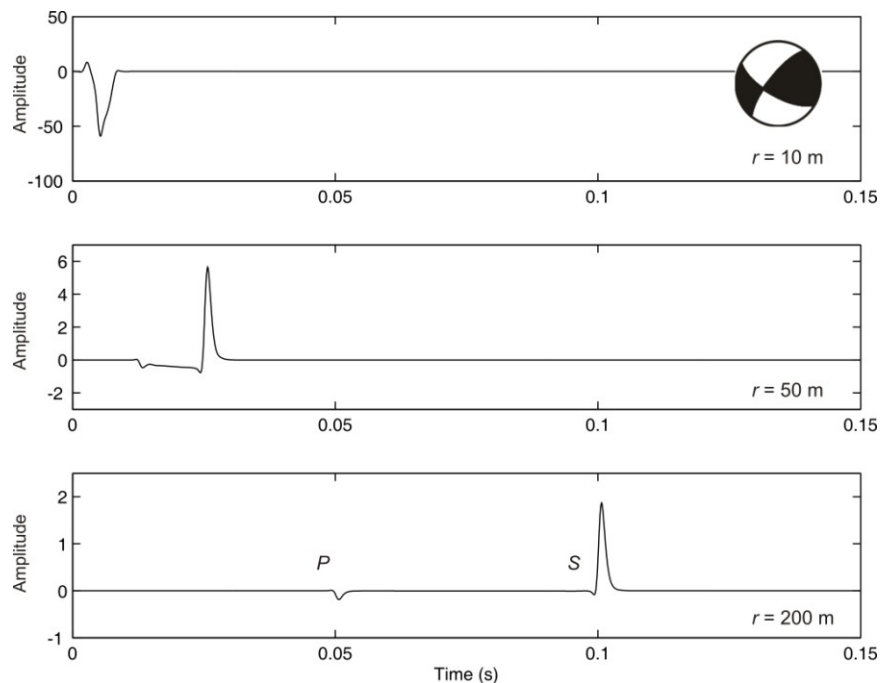
Fig. 3. Waveforms calculated using equation (7), containing both near- and far-field terms. Near-field terms dominate at a distance of 10 m, which is within about 1 seismic wavelength of the source. Note changes in amplitude scale. Inset shows double-couple source mechanism.

Conclusions

Simple formulas from earthquake seismology provide the basis for computing theoretical source spectra and source parameters, such as corner frequency and Brune source radius. Knowledge of these parameters might provide useful insights into physical features of hydrofrac well treatments, such as fracture half length and inherent strength of the slip system. Our calculations suggest that the necessary observations (corner frequency, seismic moment) could be achieved for large events (or slip on very weak systems) using borehole microseismic systems. The second part of this paper examines the potential effects of near-field source terms on microseismic recordings. For observations made within a few seismic wavelengths of the source (e.g., if the same well were used by both observations and hydrofrac treatment), near-field effects can cause significant distortion and polarity changes to the pulse.

Acknowledgements

References

Aki, K. and P. Richards (1980). Quantitative Seismology: Theory and Methods. W.H. Freeman and Company, San Francisco.

Beresnev, I., 2001, What we can and cannot learn about earthquake sources from the spectra of seismic waves: Bulletin of the Seismological Society of America, 91, 397–400.

Brune, J. N., 1970, Tectonic stress and the spectra of seismic shear waves from earthquakes: Journal of Geophysical Research, 75, 4997–5009.

Brune, J. N., 1971, Correction: Journal of Geophysical Research, 76, 5002.

Dineva, S., Eaton, D.W., Mereu, R. and Ma, S. 2007, The October 2005 Georgian Bay (Canada) earthquake sequence: Mafic dykes and their role in the mechanical heterogeneity of Precambrian crust. Bull. Seismol. Soc. Am., 97: 457-473.